APPLIED ORGANOMETALLIC CHEMISTRY
Appl. Organometal. Chem. 2006; **20**: 425–435
Published online in Wiley InterScience
(www.interscience.wiley.com) DOI:10.1002/aoc.1076

Thermodynamic and spectroscopic study of the binding of dimethyltin(IV) by citrate at 25 °C

Paola Cardiano[1], Ottavia Giuffrè[1], Lorenzo Pellerito[2], Alberto Pettignano[2], Silvio Sammartano[1]* and Michelangelo Scopelliti[2]

[1]Dipartimento di Chimica Inorganica, Chimica Analitica e Chimica Fisica, Università di Messina, Salita Sperone 31, I-98166 Messina (Vill. S. Agata), Italy
[2]Dipartimento di Chimica Inorganica e Chimica Analitica 'Stanislao Cannizzaro', Università di Palermo, Viale delle Scienze, Parco d'Orleans II, I-90128 Palermo, Italy

Received 16 February 2006; Accepted 23 March 2006

Thermodynamic (potentiometric and calorimetric) and spectroscopic (^{1}H NMR, ^{119}Sn Mössbauer) studies were performed in aqueous solution in order to characterize the interaction of dimethyltin(IV) cation with citrate ligand. Six species {$(CH_3)_2Sn(cit)^-$; $[(CH_3)_2Sn]_2(cit)_2^{2-}$; $(CH_3)_2Sn(cit)H^0$; $(CH_3)_2Sn(cit)OH^{2-}$; $[(CH_3)_2Sn]_2(cit)OH^0$; $[(CH_3)_2Sn]_2(cit)(OH)_2^-$} were found. All the species formed in this system are quite stable and formation percentages are fairly high. For example, at pH = 7.5 and $C_{(CH_3)_2Sn} = C_{cit} = 10$ mmol l^{-1}, Σ% for $[(CH_3)_2Sn]_2(cit)(OH)_2^-$ and $(CH_3)_2Sn(cit)OH^{2-}$ species reaches 65%. Overall thermodynamic parameters obtained show that the main contribution to stability is entropic in nature. Thermodynamic parameters were discussed in comparison with a simple tricarboxylate ligand (1,2,3-propanetricarboxylate). Two empirical relationships were derived from thermodynamic formation parameters. Spectroscopic results fully confirm the speciation model defined potentiometrically and show the mononuclear species to have an eq-$(CH_3)_2$Tbp structure with different arrangements around the metal, while for $[(CH_3)_2Sn]_2(cit)(OH)_2^-$ there are two different Sn(IV) environments, namely *trans*-$(CH_3)_2$ octahedral and *cis*-$(CH_3)_2$ Tbp. Copyright © 2006 John Wiley & Sons, Ltd.

KEYWORDS: thermodynamic properties; calorimetry; spectroscopy; potentiometry; dimethyltin(IV) complexes

INTRODUCTION

Organotin compounds are widely found in the natural environment as they have a tendency to accumulate in living organisms, natural waters and soils. Their presence is a consequence of their use in a broad range of industrial applications, as catalysts and as biocides.[1,2] The bioalkylation processes of inorganic tin constitute another source of organotin compounds.[3,4] Their well-known toxicity depends on the number and the nature of the alkyl groups bound to the tin(IV) atom and is directly proportional to their number. Moreover, these compounds, in apparent contradiction with their toxicity, have been found to have anticancer effects on tumour cells *in vitro*.[5–7] The impact of organotin cations is related to the form in which they are present, and in aqueous solution this impact is strictly dependent on the hydrolysis that they strongly undergo as they are Lewis acids.[8]

About 10 years ago we undertook a broad study of the speciation of mono-, di- and tri-methyltin(IV) cations and their interactions with several carboxylic ligands in aqueous solution.[8–14] We chose this class of ligand because of the presence of carboxylic groups in several ligands existing in natural waters, such as amino acids, linear and aromatic polycarboxylic acids, acidic polysaccharides, humic and fulvic substances, etc. In addition to potentiometric and calorimetric studies,[15–18] a variety of spectroscopic investigations[19] of alkyltin(IV)-containing aqueous solutions have been reported in the literature and techniques such as ^{1}H NMR, ^{13}C NMR and Mössbauer, among others, have been widely used to better understand the interactions between metal centres and various ligands.[20–22] Of all the hydrocarboxylic acids, citric acid is of particular biological importance and for this reason constitutes the basis of our investigation of the influence of the OH group on

*Correspondence to: Silvio Sammartano, Dipartmentio de Chimica Inorganica, Chimica Analitica e Chimica Fiscia, Università di Messina, Salita Sperone 31, I-98166 Messina (Vill. S. Agata), Italy.
E-mail: ssammartano@unime.it

the interaction with the metal centre. The use of capillary electrophoresis in the separation of organotin species confirmed that complexes were formed between organotin compounds and buffer anions, such as citrate.[23] Two reports in the literature[17,24] discuss potentiometric studies of the interactions between dimethyltin(IV) cation and citrate, but these include neither enthalpic data nor any examination of the spectroscopic properties of the complexes formed in aqueous solution. In this paper we have tried to give a complete picture of the influence of the alcoholic group on the interaction of dimethyltin(IV) cation with citrate by determining thermodynamic parameters, describing solution speciation and confirming findings by spectroscopic (^{1}H NMR and ^{119}Sn Mössbauer) investigation.

EXPERIMENTAL

Materials

Fresh dimethyltin(IV) solutions were prepared every day by weighing dichloride salt (Fluka product), twice re-crystallized before use. Anhydrous citric acid (puriss. >99.5%) and trisodium citrate dihydrate (microselected >99.5%) (Fluka products) were used without further purification and their purities, which were always higher than 99.5%, were checked by potentiometric titrations with standard solutions of NaOH and HCl, respectively. Sodium hydroxide and hydrochloric acid solutions were prepared by diluting concentrated Fluka ampoules and were standardized against potassium biphthalate and sodium carbonate, respectively. All the solutions were prepared using analytical grade water (resistivity = 18 MΩ cm) and grade A glassware.

Potentiometric apparatus and procedure

Potentiometric titrations were carried out (at 25.0 ± 0.1 °C) using apparatus consisting of a model 713 Metrohm potentiometer, equipped with a combined glass electrode (Ross type 8102, from Orion) and a Model 765 Metrohm motorized burette. Estimated accuracy was ±0.2 mV and ±0.003 ml for e.m.f. and titrant volume readings, respectively. The apparatus was connected to a PC, and automatic titrations were performed using a suitable computer program to control titrant delivery, data acquisition and to check for e.m.f. stability. All titrations were carried out under magnetic stirring and presaturated N_2 was bubbled through the purified solution in order to exclude O_2 and CO_2 inside. A volume of 25 ml of the solution containing the citric acid (cit) and the dimethyltin(IV) dichloride was titrated with standard NaOH up to 80–90% neutralization. Titrations were performed without adding background salt. Details of experimental measurements are reported in Table 1. Separate titrations of HCl at the same ionic strength as the sample under study were carried out to determine standard electrode potential E^0 and to obtain $pH = -\log[H^+]$ readings. The junction potential was also considered using the simple linear term $E_j = j_a\ [H^+]$ (E_j = junction potential; j_a = empirical coefficient calculated in the calibration titrations). The reliability of the calibration in the alkaline range was checked by calculating pK_w values.

Calorimetric equipment and procedure

The measurements were carried out using a model 450 Tronac Isoperibolic Titration calorimeter, coupled with a Keithley 196 system Dmm digital multimeter. A volume of 50 ml of solution, containing dimethyltin(IV) dichloride at 25.000 ± 0.001 °C, was titrated with a solution of Na_3cit. Details of experimental measurements are reported in Table 1. The titrant was delivered by a 2.5 ml capacity Hamilton syringe, model 1002TLL. A computer program was used for the acquisition of calorimetric data. Accuracy was checked by titrating a THAM [tris-(hydroxymethyl)amino-methane] buffer with HCl. The heat of dilution was measured before each experiment. The accuracy of the calorimetric apparatus was $Q \pm 0.008$ J and $v \pm 0.001$ cm^3.

NMR measurements

^{1}H NMR spectra were recorded on Bruker AMX R-300 and Avance DRX 500 spectrometers. The chemical shifts were measured with respect to dioxane, which was used as an internal reference, and converted relative to TMS using $\delta_{dioxane} = 3.70$ ppm. For ^{1}H measurements, the concentration of both citrate and dimethyltin(IV) cation was 10 mmol l^{-1}. Measurements were generally carried out in a 9:1 H_2O:D_2O mixture. In order to calculate the individual chemical shifts and $^2J(^{119}Sn-^1H)$ coupling constants of the different species, the ^{1}H NMR spectra were recorded at different pH values between 3 and 9. The individual NMR parameters (δ, ^2J) belonging both to the hydrolysed species of dimethyltin(IV) and to the dimethyltin(IV)–citrate complexes were calculated assuming fast mutual exchange.[25] The heteronuclear couplings relative to tin-bound methyl groups $^2J(^{119}Sn-^1H)$ determined in this way were converted into C–Sn–C angles according to the published equation.[26]

Table 1. Experimental conditions for potentiometric and calorimetric measurements (T = 25 °C)

Potentiometric measurements	$C_{(CH_3)_2SnCl_2}$ [a]	C_{H_3cit} [a]	I [a,b]	N_{tit} [c]	N_{pts} [d]
	0.002	0.003	0.015	3	248
	0.004	0.005	0.016	4	384
	0.002	0.006	0.015	3	296
Calorimetric measurements	$C_{(CH_3)_2SnCl_2}$ [a]	C_{Na_3cit} [a]	I [a,b]	N_{tit} [c]	N_{pts} [d]
	0.002	0.2509	0.013	3	120
	0.002	0.2509	0.010	3	120

[a] Concentrations in mol l^{-1}; [b] mean value of ionic strength; [c] number of titrations; [d] number of points.

DOI: 10.1002/aoc

Mössbauer measurements

The ^{119}Sn Mössbauer spectra of quick-frozen solutions (measured in a pH range 5–7) were obtained with a $Ca^{119}SnO_3$ (10 mCi, Ritverc GmbH, Saint Petersburg, Russian Federation) source at room temperature. The absorber samples of the $(CH_3)_2Sn$(IV) derivatives investigated at concentration 10 mmol l^{-1} were contained in cylindrical polythene sample holders (~1 ml, 1 cm^2 cross-section, corresponding to 0.10 mg ^{119}Sn cm^{-2}) and maintained at liquid nitrogen temperature, 77.3 ± 0.1 K. The source motion was effected by Wissenschaftliche Elektronik GmbH apparatus (Germany). Velocity calibration was carried out with an enriched iron foil spectrum ($^{57}Fe = \alpha - ^{57}Fe$, thickness 4 μm, Ritverc GmbH, Saint Petersburg, Russian Federation) at room temperature, using a ^{57}Co source (10 mCi, Ritverc GmbH, Saint Petersburg, Russian Federation) in a Rhodium matrix, while the zero point of Doppler velocity was determined at room temperature via the absorption spectrum of natural $CaSnO_3$ containing 0.5 mg cm^{-2} of ^{119}Sn; 5×10^5 counts were collected for each velocity point.

Calculations

All the parameters relative to alkalimetric purity determination were refined using the nonlinear least squares computer program ESAB2M. Formation constants were refined using the nonlinear least squares computer programs STACO and BSTAC. Speciation profiles were obtained using the computer program ES4EC. Details of calculation methods and programs have already been reported.[27] All the concentration and complex formation data are given in the molar (mol l^{-1}) scale. Errors are given as standard deviations.

No background salt was added to the solutions under study in order to avoid interferences. Therefore the potentiometric measurements were carried out at low and variable ionic strength. Interactions of dimethyltin(IV) with small amounts of Cl^- from the dimethyltin(IV) dichlorides and of citrate anion with small amounts of Na^+ from the standard NaOH titrant were taken into account in the calculations. Formation constants were corrected to zero ionic strength as already reported.[28,29] Both BSTAC and STACO computer programs can deal with potentiometric data obtained in variable ionic strength conditions and perform corrections to $I = 0$ mol l^{-1}. All the formation data were extrapolated to infinite dilution. The dependence on ionic strength of formation constants was taken into account using the Debye–Hückel type equation:

$$\log \beta = \log^{T} \beta - z^* \sqrt{I}/(2 + 3\sqrt{I}) + CI + DI^{3/2} \qquad (1)$$

where

$$C = c_0 p^* + c_1 z^*;\ D = d_1 z^*;\ p^* = \Sigma p_{\text{reactants}} - \Sigma p_{\text{products}};$$
$$z^* = \Sigma z^2_{\text{reactants}} - \Sigma z^2_{\text{products}}$$

(β = formation constant; $^{T}\beta$ = formation constant at zero ionic strength; and p and z are stoichiometric coefficients and charges, respectively). The results of a series of investigations showed that, when all interactions are taken into account, the empirical parameters of eq. (1) for $I \leq 1$ mol l^{-1} are given by $c_0 = 0.11$, $c_1 = 0.20$ and $d_1 = -0.075$.[28,29] At $I < 0.05$, $\sigma(\log \beta) \approx 0.15\ I$ and therefore, since the ionic strength in our measurements was always less than 0.020 mol l^{-1}, the contribution to total error of this extrapolation procedure is less than 0.003 log units.

Calorimetric titration data were analysed by the computer program ES5CM.[30] NMR calculations were performed using the general linear and nonlinear least squares computer program LIANA.[27]

Mössbauer data were refined with appropriate model with GNUPlot software, which uses least squares non linear curve fitting to obtain Mössbauer isomer shift parameters, δ (mm s^{-1}), and nuclear quadrupole splitting, Δ (mm s^{-1}), for the complexes investigated. The approximate extent of distortion from the octahedral idealized structures may be calculated using the Sham and Bancroft model and ignoring the contribution to the electric field gradient (e.f.g.) of all atoms except the carbon atoms of the organic groups bonded to the tin atoms.[31] C–Sn–C may be calculated as $(180 - 2\theta)$, θ being calculated according to the equation:

$$\Delta = 4\{\text{Alk}\}[1 - 3\cos^2\theta \text{sen}^2\theta]1/2$$

where {Alk} is the partial quadrupole splitting of the methyl group in an idealized octahedral configuration (namely, {Alkyl} = −1.03 mm s^{-1}).[32–36]

Furthermore, the experimental $|\Delta_{exp}|$ values were compared with the calculated ones (Δ_{cal}), assuming different stereochemistries of the coordination sphere of tin(IV), according to the point charge model formalism.[37,38] The partial quadrupole splitting (pqs) values of the functional groups used in the calculations are listed in the footnote to the relative table.[34,39]

RESULTS AND DISCUSSION

Potentiometric and calorimetric measurements

The protonation of citric acid and the formation of complexes with Na^+ have already been studied.[40] Table 2

Table 2. Thermodynamic parameters for protonation and Na^+ complex formation of citric acid at $T = 25$ °C and $I = 0$ mol l^{-1}

pqr	$\log \beta^{a,b}$	$\Delta H^{0b,c}$
011	6.42	1.6
012	11.17	−2.5
013	14.30	7.9
110	1.54	3.0
111	7.29	−2.7
210	2.34	−4.7

[a] Reaction: $pNa^+ + qL^{3-} + rH^+ = Na_pL_qH_r^{(p+r-3q)}$. [b] Ref. 40.
[c] Expressed in kJ mol^{-1}.

DOI: 10.1002/aoc

shows $\log\beta$ and ΔH^0 values at $I = 0$ mol l^{-1} and $T = 25$ °C. Dimethyltin(IV) cation shows a strong tendency to hydrolysis in aqueous solution, forming five hydrolytic species [$(CH_3)_2Sn(OH)^+$; $(CH_3)_2Sn(OH)_2{}^0$; $(CH_3)_2Sn(OH)_3{}^-$; $[(CH_3)_2Sn]_2(OH)_2{}^{2+}$; $[(CH_3)_2Sn]_2(OH)_3{}^+$], whose equilibrium constants and hydrolysis enthalpies are reported in Table 3 together with thermodynamic parameters for complexes with Cl^-; the mononuclear species are predominant with very high formation percentages while binuclear species are formed in fairly low percentages. Analysis of potentiometric data of the $(CH_3)_2Sn$–citrate system shows that six species: $(CH_3)_2Sn(cit)^-$; $[(CH_3)_2Sn]_2(cit)_2{}^{2-}$; $(CH_3)_2Sn(cit)H^0$; $(CH_3)_2Sn(cit)OH^{2-}$; $[(CH_3)_2Sn]_2(cit)OH^0$; and $[(CH_3)_2Sn]_2(cit)(OH)_2{}^-$ are formed. Several trials were performed, using different sets of complex species, in order to find the best speciation model. Some calculation details are reported in Table 4. Table 5 gives overall thermodynamic parameters, including ΔH^0 and $T\Delta S^0$, at infinite dilution. The overall enthalpies obtained by calorimetric measurements were mainly endothermic and errors were within acceptable limits, except for $[(CH_3)_2Sn]_2(cit)_2{}^{2-}$ species. The main contribution to stability is entropic in nature. The partial thermodynamic parameters in Table 6 refer to the most probable formation reaction. For the mononuclear species log$K$ values range from 3.59 to 4.15; this means that the species formed are quite stable. The most probable formation reaction was hypothesized on the basis of the species present at maximum (approximated) formation percentage in the systems containing only citrate or dimethyltin(IV). ΔH^0 for partial equilibria (Table 6) show an opposite trend with respect to those for the overall formation reaction: in this case the main contribution to

Table 3. Thermodynamic parameters for hydrolysis and Cl^- complex formation of $(CH_3)_2Sn^{2+}$ at $T = 25$ °C and $I = 0$ mol l^{-1}

pqr	$\log\beta$[a,b]	ΔH^0[c,d]
10–1	−2.86	33.1
10–2	−8.16	62.1
10–3	−19.35	97.7
20–2	−4.99	60.0
20–3	−9.06	85.0
11 0	0.78	—
11–1	−3.17	—

[a] Reaction: $pM^{2+} + qCl^- + rH_2O = M_pCl_q(OH)_r{}^{2p-(r+1)} + rH^+$. [b] Refs 8 and 10. [c] Expressed in kJ mol^{-1}. [d] Ref. 46.

Table 4. Some trials for the selection of the best speciation model

Species	log β[a]				
$(CH_3)_2Sncit$	7.711 ± 0.006[b]	7.771 ± 0.004[b]	7.887 ± 0.002[b]	8.021 ± 0.004[b]	8.033 ± 0.003[b]
$(CH_3)_2SncitH$	12.348 ± 0.001	12.346 ± 0.001	12.375 ± 0.002	12.352 ± 0.003	12.354 ± 0.003
$[(CH_3)_2Sn]_2citOH$	8.436 ± 0.008	8.39 ± 0.01	—	—	—
$[(CH_3)_2Sn]_2cit(OH)_2$	3.854 ± 0.003	3.833 ± 0.003	3.746 ± 0.003	—	—
$(CH_3)_2SncitOH$	1.853 ± 0.004	1.864 ± 0.003	1.933 ± 0.003	2.141 ± 0.006	2.219 ± 0.004
$[(CH_3)_2Sn]_2(cit)_2$	17.43 ± 0.02	—	—	—	—
$(CH_3)_2Sn(cit)_2$	—	—	—	10.70 ± 0.03	—
σ[c]	1.553	1.583	2.085	5.782	6.339
ε[d]	0.768	0.783	0.979	2.238	2.521
$\sigma^2/\sigma_0{}^2$[e]		1.039	1.802	13.862	16.661

[a] Overall formation constants. [b] Standard deviation. [c] Standard deviation on the fit (weighted residuals). [d] Mean deviation on the fit. [e] Variance ratio.

Table 5. Overall thermodynamic formation parameters[a] of $(CH_3)_2Sn$–citrate complexes, at $T = 25$ °C and $I = 0$ mol l^{-1}

Species	$\log\beta \pm 3s$[b]	$-\Delta G^0$[c]	$\Delta H^0 \pm s$[b,c]	$T\Delta S^0$[c]
$(CH_3)_2Sn(cit)^-$	7.71 ± 0.02	44.0	5.6 ± 0.5	50
$[(CH_3)_2Sn]_2(cit)_2{}^{2-}$	17.43 ± 0.06	99.5	45 ± 1	144
$(CH_3)_2Sn(cit)H^0$	12.348 ± 0.003	70.5	5.0 ± 0.5	75
$(CH_3)_2Sn(cit)OH^{2-}$	1.85 ± 0.01	10.6	−2.6 ± 0.5	8
$[(CH_3)_2Sn]_2(cit)OH^0$	8.44 ± 0.03	48.2	54.5 ± 0.5	103
$[(CH_3)_2Sn]_2(cit)(OH)_2$	3.854 ± 0.009	22.0	59.5 ± 0.5	81

[a] According to the reaction: $p(CH_3)_2Sn^{2+} + qcit^{3-} + rH_2O = [(CH_3)_2Sn]_pcit_q(OH)_r{}^{(2p-3q-r)} + rH^+$. [b] s = standard deviation. [c] Expressed in kJ mol^{-1}.

DOI: 10.1002/aoc

Table 6. Partial thermodynamic formation parameters of $(CH_3)_2Sn$–citrate complexes, at $T = 25\,^{\circ}C$ and $I = 0$ mol l^{-1}

Equilibrium	log$K$	$-\Delta G^{0a}$	ΔH^{0a}	$T\Delta S^{0a}$
$Hcit^{2-} + (CH_3)_2Sn(OH)^+ = (CH_3)_2Sn(cit)^- + H_2O$	4.15	23.7	−29	−5
$2Hcit^{2-} + 2(CH_3)_2Sn(OH)^+ = [(CH_3)_2Sn]_2(cit)_2{}^{2-} + 2H_2O$	10.31	58.8	−24	35
$H_2cit^- + (CH_3)_2Sn(OH)^+ = (CH_3)_2Sn(cit)H^0 + H_2O$	4.04	23.1	−26	−3
$Hcit^{2-} + (CH_3)_2Sn(OH)_2{}^0 = (CH_3)_2Sn(cit)OH^{2-} + H_2O$	3.59	20.5	−66	−45
$Hcit^{2-} + 2(CH_3)_2Sn(OH)^+ = [(CH_3)_2Sn]_2(cit)OH^0 + H_2O$	7.74	44.2	−13	31
$cit^{3-} + 2(CH_3)_2SnOH^+ = [(CH_3)_2Sn]_2(cit)(OH)_2{}^-$	9.57	54.6	−7	48

[a] Expressed in kJ mol^{-1}.

stability is enthalpic in nature. This is due to the formation of H_2O ($\Delta H^0{}_w = -55.5$ kJ mol^{-1} at $I = 0$ mol l^{-1} and $T = 25\,^{\circ}C$). For the formation of the species containing two molecules of dimethyltin(IV), $[(CH_3)_2Sn]_2(cit)_2{}^{2-}$, $[(CH_3)_2Sn]_2(cit)OH^0$, $[(CH_3)_2Sn]_2(cit)(OH)_2{}^-$, $T\Delta S^0 > (-\Delta H^0)$, particularly for the last one, where no H_2O molecule is formed. It is also interesting to note that for the dimerization reaction

$$2(CH_3)_2Sn(cit)^- = [(CH_3)_2Sn]_2(cit)_2{}^{2-}$$

$$\Delta G^0 = -11.5 \qquad \Delta H^0 = 34 \qquad T\Delta S^0 = 44$$

i.e. the dimerization process is endothermic, as for many metal complexes.

Figure 1 (A) shows the distribution of the species $(CH_3)_2Sn^{2+}$-citrate vs pH. As can be seen when $C_{(CH_3)_2Sn} = C_{cit} = 10$ mmol l^{-1}, percentages are quite significant in the range $2 \le pH \le 8$. The sum of percentages for these species (except the hydrolytic ones), in the range $3 \le pH \le 6$, is about 90%. In the acid range $2 \le pH \le 4$ the predominant species is $(CH_3)_2Sn(cit)H^0$, with log $K = 4.04$ and formation percentage higher than 70%, while the hydrolytic species $(CH_3)_2Sn(OH)^+$, which predominates in the absence of citrate, only reaches a percentage of 8%. In the range $4.5 \le pH \le 7.5$ the species that reaches the highest formation percentage (68%) is $[(CH_3)_2Sn]_2(cit)(OH)_2{}^-$.

A comparison of the distribution diagrams relative to the $(CH_3)_2Sn$–citrate and $(CH_3)_2Sn$–1,2,3-propanetricarboxylate (tricarballylate, tca)[12] systems represented in Figs 1(A) and 2, respectively, reveals a number of differences: (1) the formation percentages reached by $(CH_3)_2Sn$–citrate species are higher than those relative to the $(CH_3)_2Sn$–tricarballylate system; (2) in the pH range 7–8, of particular interest for natural waters, Σ% of the $[(CH_3)_2Sn]_2(cit)(OH)_2{}^-$ and $(CH_3)_2Sn(cit)OH^{2-}$ species are also significant; a formation percentage of 65% is reached at $C_{(CH_3)_2Sn} = C_{cit} = 10$ mmol l^{-1}

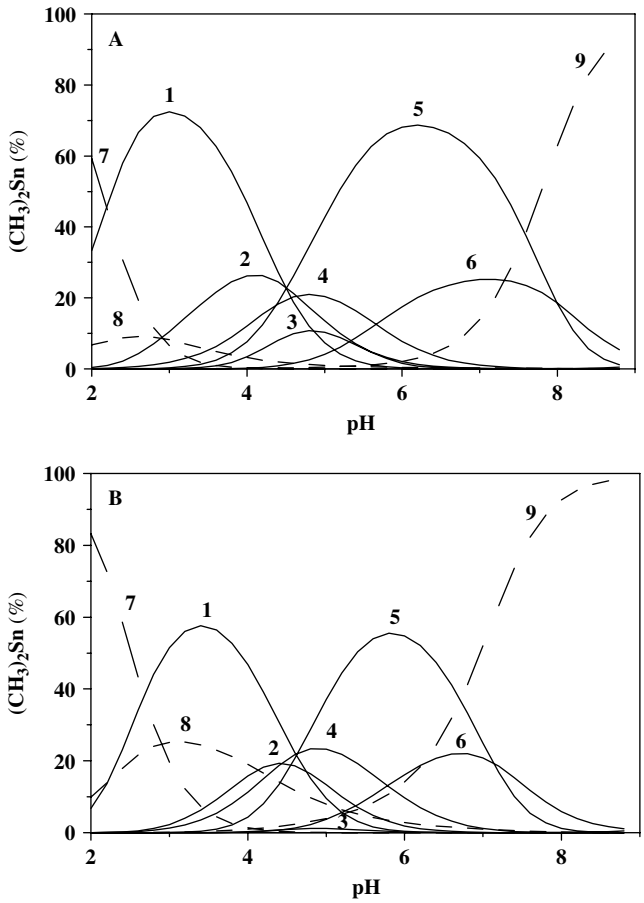

Figure 1. Distribution diagrams of $(CH_3)_2Sn^{2+}$ cation-citrate *vs.* pH at $T = 25\,^{\circ}C$. Species: 1, $(CH_3)_2Sn(cit)H^0$; 2, $[(CH_3)_2Sn]_2(cit)OH^0$; 3, $[(CH_3)_2Sn]_2(cit)_2{}^{2-}$; 4, $(CH_3)_2Sn(cit)^-$; 5, $[(CH_3)_2Sn]_2(cit)(OH)_2{}^-$; 6, $(CH_3)_2Sn(cit)OH^{2-}$; 7, $(CH_3)_2Sn^{2+}$; 8, $(CH_3)_2Sn(OH)^+$; 9, $(CH_3)_2Sn(OH)_2{}^0$. Hydrolytic species are shown by dashed lines. A: $C_{(CH_3)_2Sn} = C_{cit} = 10$ mmol l^{-1}. B: $C_{(CH_3)_2Sn} = C_{cit} = 1$ mmol l^{-1}.

and pH = 7.5 and 37% at pH = 8 [Fig. 1(A)]; at $C_{(CH_3)_2Sn} = C_{cit} = 1$ mmol l^{-1} and pH = 7.5 [Fig. 1(B)] Σ% for complex species is 21%, which is still considerable. On the other hand, for the tricarballylate system in the same pH range and at $C_{(CH_3)_2Sn} = C_{tca} = 10$ mmol l^{-1}, only $(CH_3)_2Sn(tca)OH^{2-}$ species is observed to reach very low formation percentages, in particular 9% at pH = 7.5 and 3% at pH = 8. This confirms that in the pH range 7–8, and at $C_{(CH_3)_2Sn} = C_L =$ 1–10 mmol l^{-1}, only $(CH_3)_2Sn$-citrate species are significant, due to the additional OH group able to promote the formation of complexes even at pH = 8; this has interesting implications for the study of the interactions of humic substances, which both have —OH and —COOH groups in their molecules.

For purposes of comparison, Table 7 shows the findings of Ref. 17, obtained for $(CH_3)_2Sn$(IV)-citrate systems at $I =$ 0.1 mol l^{-1} in KNO_3 and recalculated by us at $I = 0$ mol l^{-1}, using an equation similar to eqn (1) and the empirical

DOI: 10.1002/aoc

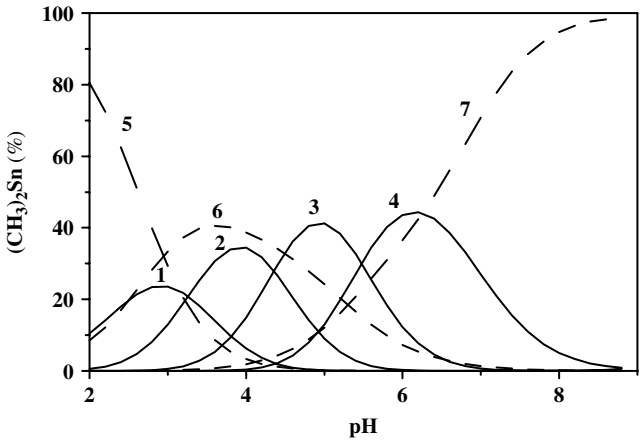

Figure 2. Distribution diagrams of $(CH_3)_2Sn^{2+}$ cation-tricarballylate (tca) vs pH at $T = 25\,^{\circ}C$. Species: 1, $(CH_3)_2Sn(tca)H_2^{+}$; 2, $(CH_3)_2Sn(tca)H^{0}$; 3, $(CH_3)_2Sn(tca)^{-}$; 4, $(CH_3)_2Sn(tca)OH^{2-}$; 5, $(CH_3)_2Sn_2^{2+}$; 6, $(CH_3)_2Sn(OH)^{+}$; 7, $(CH_3)_2Sn(OH)_2^{0}$. Hydrolytic species are shown by dashed lines. $C_{(CH_3)_2Sn} = C_{tca} = 10$ mmol l^{-1}.

coefficients reported in Refs 28 and 29. As can be seen, the differences are minimal, with a maximum $\Delta \log \beta = 0.10$ for the $[(CH_3)_2Sn]_2(cit)OH^0$ and $(CH_3)_2Sn(cit)^-$ species. We did, however, identify a new species, $[(CH_3)_2Sn]_2(cit)_2^{2-}$. The same table shows values for this system with another tricarboxylate ligand (tricarballylate), whose equilibrium constants are reported in Ref. 12. In this system, under experimental conditions comparable to those used in this study, no polynuclear species are formed and the equilibrium constant values relative to the mononuclear species are considerably lower than those of the citrate system, as can be seen in Fig. 2. For example the species $(CH_3)_2SnLH^0$ is characterized by a $\Delta(\log \beta_{cit} - \log \beta_{tca}) = 1.23$; this higher stability is undoubtedly connected to the presence of the –OH group in the citrate, which gives rise to further interactions with $(CH_3)_2Sn^{2+}$.

As no enthalpic values for dimethyltin(IV)–tricarboxylate complexes had previously been reported, we compared these data with the results we obtained with the tricarballylate ligand (Table 8) and found enthalpic and entropic values to be more discriminant than stability values, while values for tricarballylate proved markedly more positive than those for citrate. On the other hand, comparison of the thermodynamic parameters of dimethyltin(IV)–citrate complexes with those of the same ligand with a series of divalent transition metals, such as Cu, Ni, Zn and Cd, shows, as reported in Table 9, that the stability of the former is markedly higher than the latter series, owing to the different nature of the metals, while enthalpy values are broadly comparable, except for $[(CH_3)_2Sn]_2(cit)_2^{2-}$ species.

Two empirical equations can be derived from thermodynamic formation parameters. The first is based on the well-known correlation between ΔG^0 and $T\Delta S^0$,[41,42] and for

Table 7. Literature comparisons, at $T = 25\,^{\circ}C$ and $I = 0$ mol l^{-1}

	logβ		
Species	L = citrate, this work	L = citrate,[a] Ref. 17	L = tricarballylate, Ref. 12
$(CH_3)_2SnL^-$	7.71	7.81	6.69
$[(CH_3)_2Sn]_2L_2^{2-}$	17.43	—	—
$(CH_3)_2SnLH^0$	12.348	12.31	11.12
$(CH_3)_2SnLH_2^+$	—	—	14.38
$(CH_3)_2SnLOH^{2-}$	1.85	1.83	1.01
$[(CH_3)_2Sn]_2LOH^0$	8.44	8.34	—
$[(CH_3)_2Sn]_2L(OH)_2^-$	3.854	3.86	—

[a] Recalculated from values at $I = 0.1$ mol l^{-1} in KNO_3 using an equation similar to eqn (1), with empirical coefficients reported in Refs 28 and 29.

Table 8. Comparison between overall thermodynamic formation parameters[a] of $(CH_3)_2Sn$–citrate and $(CH_3)_2Sn$–tricarballylate complexes, at $T = 25\,^{\circ}C$ and $I = 0$ mol l^{-1}

	Citrate[b]		Tricarballylate[c]	
	ΔH^0	$T\Delta S^0$	ΔH^0	$T\Delta S^0$
$(CH_3)_2SnLH^0$	5.0	75	30.7	94
$(CH_3)_2SnL^-$	5.6	50	44.7	83
$(CH_3)_2SnLOH^{2-}$	−2.6	8	45.1	51

[a] Expressed in kJ mol^{-1}. [b] This work. [c] Values from a work in progress from this laboratory.

Table 9. Comparison with the stability of other metal ions at $T = 25\,^{\circ}C$

	logβ				
Species	$(CH_3)_2Sn^{2+}$[a]	Cu^{2+}[b,c]	Ni^{2+}[b,c]	Zn^{2+}[b,d]	Cd^{2+}[b,d]
$M(cit)^-$	7.71	—	5.35	5.02	3.71
$M(cit)H^0$	12.348	9.55	9.13	8.71	7.85
$M_2(cit)_2^{2-}$	17.43	14.43			
	ΔH^{0e}				
$M(cit)^-$	5.6		13	8	8
$M(cit)H^0$	5.0	9	9	1	1
$M_2(cit)_2^{2-}$	45	28			

[a] At $I = 0$ mol l^{-1}. [b] At $I = 0.1$ mol l^{-1} in KNO_3. [c] Ref. 47. [d] Ref. 48. [e] Expressed in kJ mol^{-1}.

cit-$(CH_3)_2Sn$(IV) complexes we can write

$$\frac{T\Delta S^0 - 9.5}{\Delta G^0} = -1.3 \pm 0.1 \qquad (2)$$

DOI: 10.1002/aoc

Although the fit of data in Table 5 to eqn (2) is quite poor, it is interesting that the coefficient 1.3 ± 0.1 is in very good agreement with previous findings for a number of other systems.[43] Moreover, ΔG^0_{pqr}, which refers to the equilibrium reaction

$$pM^{2+} + qL^{3-} + rH_2O \rightleftharpoons M_pL_q(OH)_r^{(2p-3q-r)} + rH^+ \quad (3)$$

can be expressed as a linear combination of stoichiometric coefficients according to the equation

$$-\Delta G^0_{pqr}(\pm 1.4) = 40.35p + 59.40(q + r/2 - 1) \quad (4)$$

where the number of H in the species formed was assumed to be $r > 0$ and the number of OH to be $r < 0$. The simple two-parameter eqn (4) is an excellent representation of experimental data as shown in Fig. 3.

NMR and Mössbauer measurements

In order to obtain information about the spectroscopic properties of the dimethyltin(IV)–citrate complexes, ^{1}H, ^{119}Sn and ^{13}C NMR investigations were carried out. Regardless of experimental conditions (i.e. concentrations of precursors, pH) all the dimethyltin(IV)–cit species involved in the equilibria showed a fast mutual exchange over the whole pH range studied; as a consequence, direct measurement of individual NMR parameters cannot be performed. As far as ^{1}H NMR investigations are concerned, the spectra for both pure dimethyltin(IV) and dimethyltin(IV)–citrate solutions show a single sharp signal in the CH_3 region with the satellite peaks typical of heteronuclear couplings of $^2J(^{117}Sn-^1H)$ and $^2J(^{119}Sn-^1H)$ with the two NMR active isotopes of tin (natural abundance 7.68% for ^{117}Sn and 8.59% for ^{119}Sn, respectively). In the case of pure dimethyltin(IV), both chemical shifts and the ^2J coupling constants of CH_3 protons decrease steadily with increasing pH, whilst the dimethyltin(IV)–citrate solutions do not follow the same trend, indicating the participation of the metal ion not only in hydrolysis phenomena but also in other interactions due to the action of citrate on the equilibria. Figure 4 shows variations in δCH_3 vs pH for both pure dimethyltin(IV) and dimethyltin(IV)–citrate solutions. Despite their coinciding at pH 4 and 9, the two curves are different, consistent with the formation of complex species with citrate. Furthermore, as evidenced from speciation data, for dimethyltin(IV)–tricarballylate solutions only dimethyltin(IV)–hydroxo species are present in significant amounts at pH 7.5–8. In contrast, NMR experiments show the formation of citrate-containing species at higher pHs; this further stabilization of citrate complexes may be due to the citrate OH group.[20]

Owing to fast mutual exchange, the ^{1}H spectra recorded for dimethyltin(IV)–citrate and citrate solutions show only one signal in the CH_2 region (3–2.5 ppm), making it impossible to discern the peaks due to the free ligand and the coordinated citrate. As a consequence, the pH at which dimethyltin(IV) promotes citrate deprotonation cannot be detected by direct observation of NMR spectra.[22,25]

Despite fast mutual exchange, since the distribution of complex species at different pHs is known from potentiometric data, it is possible to calculate both δ and ^2J (Table 10) for each individual complex formed at a given pH. Once individual chemical shifts have been obtained, the mean δ at each experimental pH can be recalculated on the basis of speciation curves. These 'calculated' chemical shifts were compared to the observed ones (Figs 5 and 6) in order to validate the model used for the calculation of δ for each complex formed and to confirm the model used for the interpretation of potentiometric data. Figures 5 and 6 show excellent agreement between calculated and observed chemical shifts, so NMR data are consistent with the complex species distribution obtained from potentiometric experiments. Furthermore, in order to confirm the method used for calculations, individual NMR parameters relative

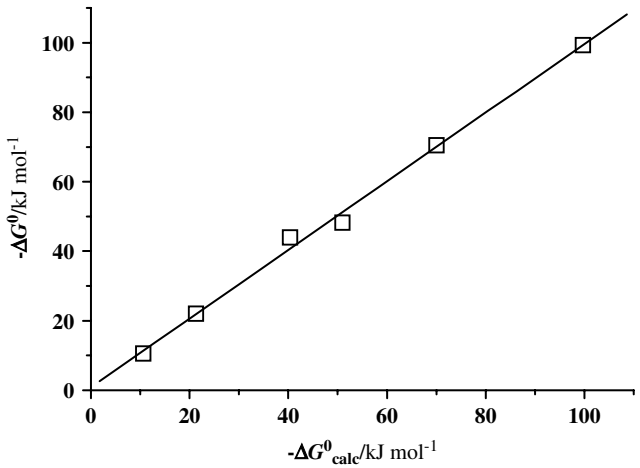

Figure 3. Overall ΔG^0 values of Table 5 vs ΔG^0 values calculated with eqn (4).

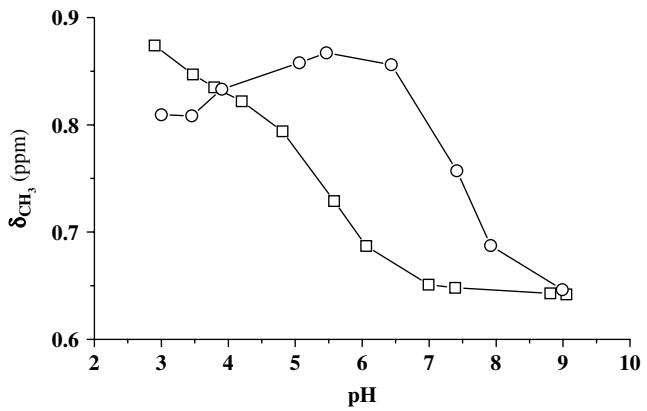

Figure 4. Measured chemical shifts of CH_3 vs. pH for: (—□—) solutions containing dimethyltin(IV) only; (—o—) dimethyltin(IV) : citrate 1 : 1 mixtures.

DOI: 10.1002/aoc

Table 10. Calculated individual ^{1}H NMR parameters

Species	$\delta(CH_3)$ (ppm)	^2J(Sn–H) (Hz)	∠ C–Sn–C (°)
$(CH_3)_2Sn(cit)^-$	0.897	80.8	131
$(CH_3)_2Sn(cit)H^0$	0.805	84.6	136
$(CH_3)_2Sn(cit)OH^{2-}$	0.580	64.8	116
$[(CH_3)_2Sn]_2(cit)(OH)_2$	0.957	86.0	138
$[(CH_3)_2Sn]_2(cit)OH^0$	0.827	94.8	151
$[(CH_3)_2Sn]_2(cit)_2^{2-}$	0.576	n.d.[a]	n.d.[a]
$(CH_3)_2Sn^{2+}$	0.920	109	180
$(CH_3)_2SnOH^+$	0.781	92.3	147
$(CH_3)_2Sn(OH)_2^0$	0.637	82.1	133
$(CH_3)_2Sn(OH)_3^-$	0.447	83.0	134

[a] Not detected.

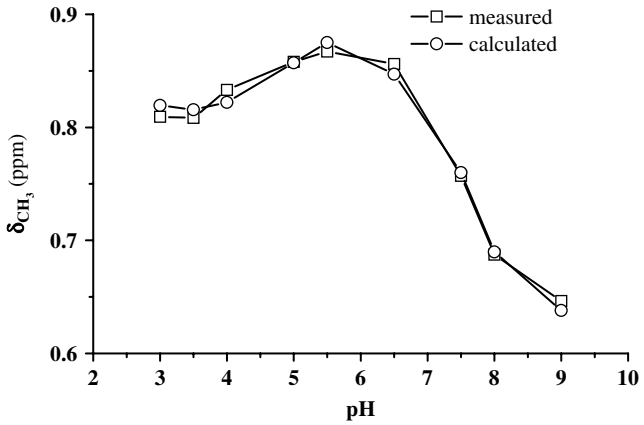

Figure 5. Chemical shifts of CH_3 vs pH in dimethyltin(IV) : citrate 1 : 1 mixtures.

to $[(CH_3)_2Sn]_p(OH)_r$ species were compared with literature data derived from the same calculation procedure,[25] despite our spectra being registered in the absence of an ionic medium, at very low ionic strength (while literature data refer to $NaClO_4$ 0.1 mol l^{-1} aqueous solutions), there is excellent agreement between the two data sets, in terms of both chemical shifts and coupling constants, and consequently also of the geometry around the metal centre.

Literature reports of $^2J(^{119}Sn-^1H)$ coupling constants of dimethyltin(IV) substrates can give qualitative information about complex geometry through the calculation of the $CH_3–Sn–CH_3$ angle.[26] Table 10 shows individual ^2J as well as calculated C–Sn–C angles for each complex formed. The calculated value of ^2J for $[(CH_3)_2Sn]_2(cit)_2^{2-}$ is characterized by a high degree of error so we do not feel confident that we can give any corresponding angle. Two reasons may be invoked to explain this result: (1) since the coupling constants ^2J were calculated on the basis of the concentrations of individual species, their values cannot be correctly evaluated for complexes formed in low percentages [i.e. in our

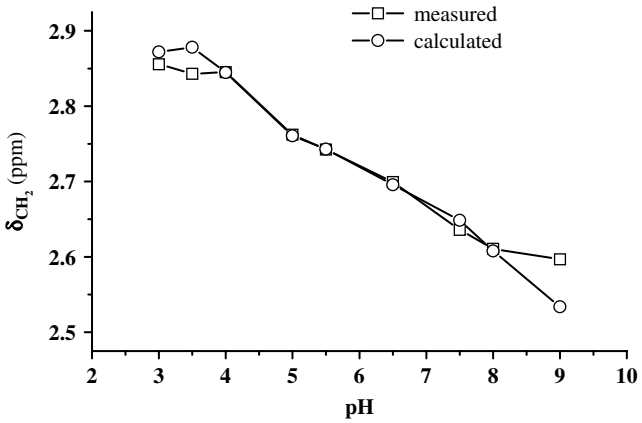

Figure 6. Chemical shifts of CH_2 vs pH in dimethyltin(IV) : citrate 1 : 1 mixtures.

experimental conditions the highest formation percentage (10.8%) for $[(CH_3)_2Sn]_2(cit)_2^{2-}$ was detected at pH ≈ 5]; (2) at certain pH values, the CH_3 signal is broadened and the ^2J medium coupling constants cannot reliably be measured from the spectrum; as a consequence, experimental ^2J values seem insufficient to obtain a good fit. Nevertheless, δ can be measured in the same conditions. As far as the $(CH_3)_2Sn(cit)OH^{2-}$ complex is concerned, the $CH_3–Sn–CH_3$ angle calculated is about 116°; this value could be explained by a trigonal bipyramidal structure with the two CH_3 groups in equatorial position,[21,44] as found for plenty of quite similar $(CH_3)_2Sn(cit)OH^{2-}$ species of dimethyltin(IV). The ^2J values calculated for the remaining species range between 131–151° suggesting a Tpb arrangement around the tin as well.

In order to obtain further information about the geometry of the complexes, ^{119}Sn Mössbauer measurements were carried out on quick-frozen solutions at selected pH values (in a 5–7 range). A comparison of the data in Tables 10 and 11, regarding NMR and Mössbauer measurements, respectively, shows good agreement between the geometries obtained by means of the two different techniques.

As far as Mössbauer measurements are concerned, the $|\Delta_{exp}|$ values of dimethyltin(IV) species were rationalized according to the point charge model formalism (p.c.f.)[34,38,45] applied to the idealized regular structures of Fig. 7(a–e).

The Δ_{calcd} values calculated are in line with experimental $|\Delta_{exp}|$ (shown in Table 11) to within less than ±0.4 mm s^{-1}, the maximum difference allowed between experimental and calculated Δ for the proposed geometry to be acceptable.[37]

A single absorbing Sn(IV) unit was present in each of the $(CH_3)_2Sn(cit)^-$ and $(CH_3)_2Sn(cit)OH^{2-}$ complexes [Fig. 7(a, b)], for which, along with the tetrahedral $(CH_3)_2Sn(OH)_2^0$ complex [Fig. 7(c)], eq-$(CH_3)_2$ Tbp structures are proposed that fully confirm NMR data. In $(CH_3)_2Sn(cit)^-$ and $(CH_3)_2Sn(cit)OH^{2-}$ complexes, citrate should behave as a bis-monodentate dianionic ligand, coordinating Sn(IV) in *cis* positions as reported in Fig. 7(a and b). Penta-coordination should be reached through coordination of an alcoholic OH or

DOI: 10.1002/aoc

Table 11. Calculated Mössbauer spectroscopic parameters of the complexes: isomer shift, δ; experimental and calculated nuclear quadrupole splittings, $|\Delta_{exp}|$ and Δ_{calcd}; and C–Sn–C angle, $\theta°$

Species[a,b]	δ (mm s^{-1})	$\lvert\Delta_{exp}\rvert$ (mm s^{-1})	Δ_{calcd} (mm s^{-1})	Geometry	$\theta°$
$(CH_3)_2Sn(cit)^-$	1.19	3.11	+3.08	Tbp	131
			+3.01		
$(CH_3)_2Sn(cit)OH^{2-}$	1.07	2.65	+2.97	Tbp	118
			+2.71		
$(CH_3)_2Sn(OH)_2{}^0$	1.10	2.45	−2.24	Td	112
$[(CH_3)_2Sn]_2(cit)OH^0$	0.95	3.67	n.c.	Tbp	148
$[(CH_3)_2Sn]_2(cit)(OH)_2{}^-$	1.26	4.00	+4.00 − 4.36	Oct	164
	1.13	3.25	+2.98 − 3.13	Tbp	135

[a] n.c. = not calculated.
[b] Partial quadrupole splitting (p.q.s., mm s^{-1}) values of the functional groups used in the calculations were: octahedral structures (Oct), $\{R\} = -1.03$, $\{COO^-\} = -0.135$; $\{OH^-\} = -0.14$, $\{ROH\} = +0.16$; trigonal bipyramidal structures (Tbp), axial (ax) or equatorial (eq), $\{R\}_{ax} = -0.94$, $\{COO^-\}_{ax} = -0.1$, $\{OH^-\}_{ax} = -0.13$, $\{ROH\}_{ax} = +0.145$; $\{R\}_{eq} = -1.13$, $\{COO^-\}_{eq} = +0.06$, $\{OH^-\}_{eq} = +0.02$, $\{ROH\}_{eq} = +0.386$; tetrahedral structures (Td):$\{R\} = -1.37$, $\{COO^-\} = +0.15$, $\{OH^-\} = -0.40$.

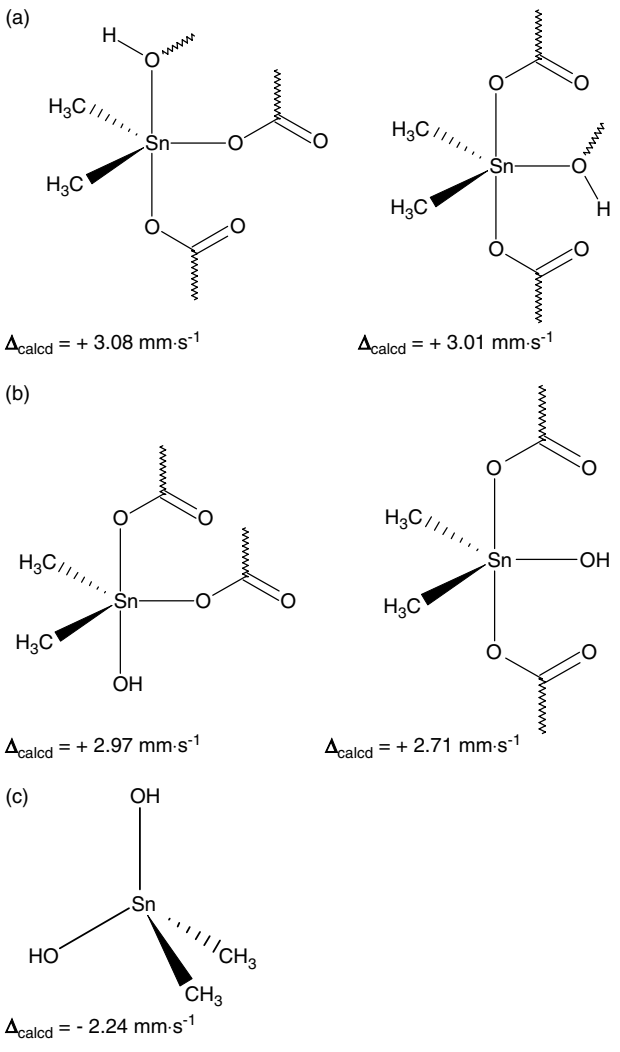

Figure 7. Proposed structures for (a) *cis*- and *trans*-$(COO^-)_2$ $(CH_3)_2Sn(cit)^-$ complex. (b) *cis*- and *trans*-$(COO^-)_2$ $(CH_3)_2$ $Sn(cit)OH^{2-}$ complex; (c) $(CH_3)_2Sn(OH)_2{}^0$; (d) $[(CH_3)_2Sn]_2(cit)$ OH^0 (n.c. = not calculated, see text); (e) $[(CH_3)_2Sn]_2(cit)(OH)_2{}^-$.

a hydroxylic OH^-, in $(CH_3)_2Sn(cit)^-$ and $(CH_3)_2Sn(cit)OH^{2-}$, respectively. Even for $(CH_3)_2Sn(cit)^-$ and $(CH_3)_2Sn(cit)OH^{2-}$ complexes it is not possible to discriminate between the *cis* and *trans* positions of the donor oxygen atoms in the carboxylate groups.

A little more complicated are the situations for $[(CH_3)_2Sn]_2(cit)OH^0$ and $[(CH_3)_2Sn]_2(cit)(OH)_2{}^-$ complexes. In fact, for $[(CH_3)_2Sn]_2(cit)OH^0$ Mössbauer spectra showed a single very intense doublet, indicative of two different tin absorbing atoms with similar environments in eq-$(CH_3)_2$ Tbp arrangements [Fig. 7(d)]. In such a complex, the citrate ligand should behave as a *tris*-monodentate trianionic bridging ligand through the oxygen atoms of ester type carboxylates. Penta-coordination of the Sn(IV) should be reached through coordination of OH^- and/or citrate OH group and/or water molecule, as shown in the two different environments reported in Fig. 7(d). Here again, Δ could not be calculated according to p.c.f. owing to the high distortion of C–Sn–C from 120°. Finally, two doublets were present in the Mössbauer spectra of $[(CH_3)_2Sn]_2(cit)(OH)_2{}^-$, whose $|\Delta_{exp}|$ were indicative of the occurrence of two different Sn(IV) environments, respectively *trans*-$(CH_3)_2$ octahedral and eq-$(CH_3)_2$ trigonal bipyramidal. It is interesting that p.c.f. calculations were not able to discriminate between several configurations in which carboxylate groups of citrate, OH^- and alcoholic OH of citrate and/or H_2O molecules could vary their positions [Fig. 7(e)], while the two Sn(IV) atoms in the complex maintained *trans*-$(CH_3)_2$ octahedral and eq-$(CH_3)_2$ trigonal bipyramidal structures.

CONCLUSION

A detailed thermodynamic and spectroscopic study was carried out of the coordination behaviour of citrate towards dimethyltin(IV) ion in aqueous solution at 25 °C. Thermodynamic formation parameters show that several species are formed in this system and that these are quite

DOI: 10.1002/aoc

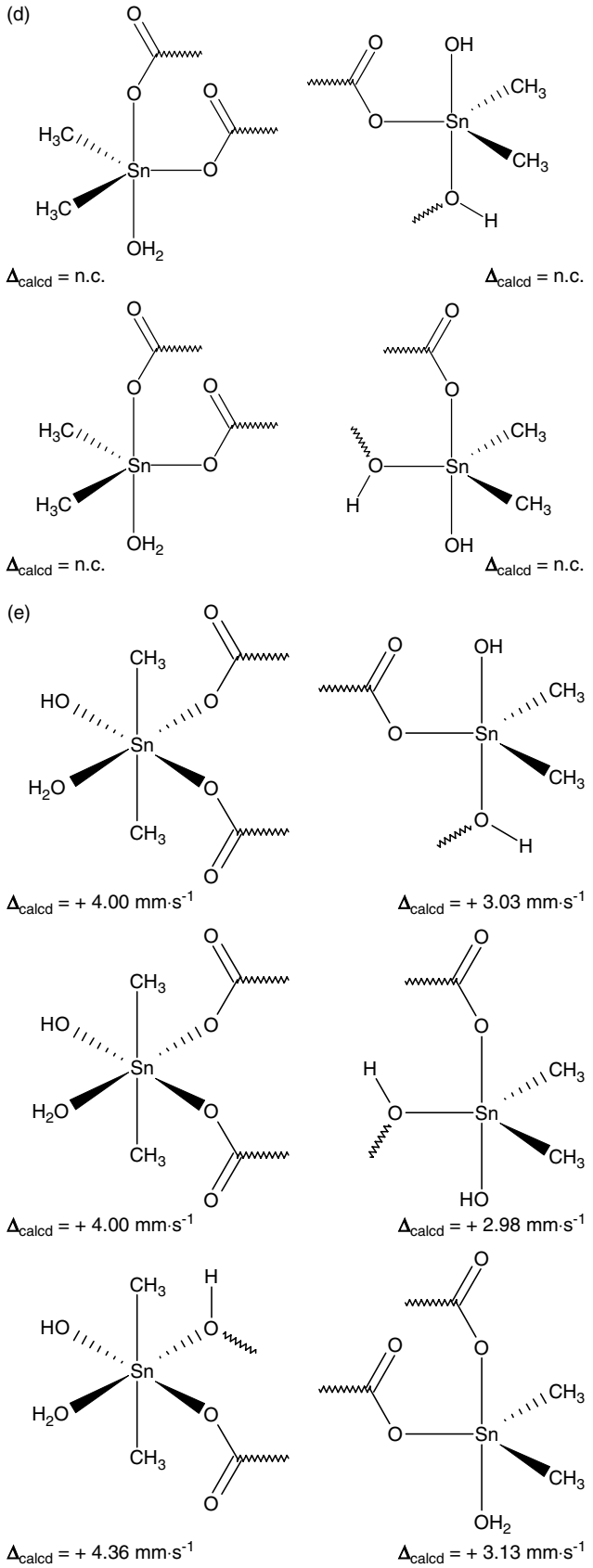

Figure 7. (*Continued*).

stable. The main contribution to stability is entropic in nature. Comparison with a simple tricarboxylate (1,2,3-propanetricarboxylate) shows that ΔG^0 values follow the trend citrate > tricarballylate. NMR investigations showed that all species involved in the equilibria are characterized by fast mutual exchange so it is not possible to identify the pH at which dimethyltin(IV) promotes citrate deprotonation. Nevertheless, individual NMR parameters can be calculated for each complex formed by taking species distribution into account at selected pH. The coupling constants obtained in this way were used to calculate C–Sn–C angles for the most abundant species in solution. The geometries proposed are in agreement with literature data for similar complexes. In addition, Mössbauer measurements were carried out in order to obtain more detailed information about the citrate arrangement around the metal. Spectroscopic data showed that $(CH_3)_2Sn(cit)^-$, $(CH_3)_2Sn(cit)OH^{2-}$, $(CH_3)_2Sn(cit)H^0$ and $[(CH_3)_2Sn]_2(cit)OH^0$ are characterized by a eq-$(CH_3)_2$ Tbp structure with different ligand arrangements around the metal, while for $[(CH_3)_2Sn]_2(cit)(OH)_2^-$ two different Sn(IV) environments were proposed, namely *trans*-$(CH_3)_2$ octahedral and *cis*-$(CH_3)_2$ Tbp. Both thermodynamic and spectroscopic measurements confirm the involvement of the –OH group in coordination.

Acknowledgements

The authors are grateful to Professor László Nagy and Prof. Tamás Gajda (Department of Inorganic and Analytical Chemistry, University of Szeged, Hungary) for some NMR measurements, and for helpful discussions. We thank University of Messina (PRA) and MURST (F.I.R.B. n. RBAU01HLFX_004), Ministerio dell'lstruzione, dell'Università e della Ricera (M.I.U.R., CIP 2004059078_003), and University of Palermo (ORPA 041443) for financial support.

REFERENCES

1. Davies AJ, Smith PJ. The synthesis, reactions and structure of organometallic compounds. In *Comprehensive Organometallic Chemistry*, Wilkinson G, Stone FGA, Abel E (eds). Pergamon Press: New York, 1982.
2. Blunden SJ, Cusack PA, Hill R. *The Industrial Use of Tin Chemicals*. The Royal Society of Chemistry: London, 1985.
3. Blunden SJ, Chapman A. Organotin compounds in the environment. In *Organometallic Compounds in the Environment*, Craig PJ (ed.). Longman: Harlow, Essex, 1986.
4. Thayer JS. Global bioalkylation of the heavy elements. In *Metal Ions in Biological Systems*, Sigel H, Sigel A (eds), Vol. 29. Marcel Dekker: New York, 1993; 1–30.
5. *Tin-Based Antitumor Drugs*. NATO ASI Series, Gielen M (ed.). Springer: Berlin, 1990.
6. Crowe AJ. *Metal-Based Antitumour Drugs*. In Gielen M (ed.), Vol. 1. Freund: London, 1989; 103–149.
7. Saxena AK, Huber F. *Coord. Chem. Rev.* 1989; **95**: 109.
8. De Stefano C, Foti C, Gianguzza A, Martino M, Pellerito L, Sammartano S. *J. Chem. Eng. Data* 1996; **41**: 511.
9. De Stefano C, Foti C, Gianguzza A, Millero FJ, Sammartano S. *J. Solution Chem.* 1999; **28**(7): 959.
10. Foti C, Gianguzza A, Piazzese D, Trifiletti G. *Chem. Spec. Bioavail.* 2000; **12**(2): 41.

DOI: 10.1002/aoc

11. De Stefano C, Foti C, Gianguzza A, Sammartano S. Hydrolysis processes of organotin(IV) compounds in seawater. In *Chemical Processes in the Marine Environment*, Gianguzza A, Pellizzetti E, Sammartano S (eds). Environmental Sciences Library. Springer: Berlin, 2000; 213–228.
12. De Stefano C, Gianguzza A, Marrone F, Piazzese D. *Appl. Organomet. Chem.* 1997; **11**: 683.
13. De Stefano C, Foti C, Gianguzza A. *Ann. Chim. (Rome)* 1999; **89**: 147.
14. Foti C, Gianguzza A, Sammartano S. *Ann. Chim. (Rome)* 2002; **92**(7–8): 705.
15. Yasuda M, Tobias RS. *Inorg. Chem.* 1963; **2**: 207.
16. Hynes MJ, O'Dowd M. *J. Chem. Soc. Dalton Trans.* 1987; 563.
17. Arena G, Contino A, Musumeci S, Purrello R. *J. Chem. Soc. Dalton Trans.* 1990; 3383.
18. Arena G, Gianguzza A, Pellerito L, Musumeci S, Purrello R, Rizzarelli E. *J. Chem. Soc., Dalton Trans.* 1990; **8**: 2603.
19. Pellerito L, Nagy L. *Coord. Chem. Rev.* 2002; **224**: 111.
20. Gajda-Schrantz K, Nagy L, Fiore T, Pellerito L, Gajda T. *J. Chem. Soc. Dalton Trans.* 2002; 152.
21. Jancsó A, Henry B, Rubini P, Vankó G, Gajda T. *J. Chem. Soc. Dalton Trans.* 2000; 1941.
22. Jancsó A, Gajda T, Szorcsik A, Kiss T, Henry B, Vankó G, Rubini P. *J. Inorg. Biochem.* 2001; **83**: 187.
23. Han F, Fasching JL, Brown PL. *J. Chromatogr. B* 1995; **669**: 103.
24. Mohanty NK, Patnaik RK. *J. Indian Chem. Soc.* 1980; **57**(8): 779.
25. Surdy P, Rubini P, Buzás N, Henry B, Pellerito L, Gajda T. *Inorg. Chem.* 1999; **38**: 346.
26. Lockhart TP, Manders WF. *Inorg. Chem.* 1986; **25**: 892.
27. De Stefano C, Sammartano S, Mineo P, Rigano C. Computer tools for the speciation of natural fluids. In *Marine Chemistry—an Environmental Analytical Chemistry Approach*, Gianguzza A, Pellizzetti E, Sammartano S (eds). Kluwer Academic: Amsterdam, 1997; 71–83.
28. Daniele PG, De Robertis A, De Stefano C, Sammartano S, Rigano C. *J. Chem. Soc. Dalton Trans.* 1985; **85**: 2353.
29. Daniele PG, De Stefano C, Foti C, Sammartano S. *Curr. Top. Sol. Chem.* 1997; **2**: 253.
30. De Robertis A, De Stefano C, Rigano C. *Thermochim. Acta* 1989; **138**: 141.
31. Sham TK, Bancroft GM. *Inorg. Chem.* 1975; **14**: 2281.
32. Bancroft GM. *Mössbauer Spectroscopy. An Introduction for Inorganic Chemists and Geochemists*. McGraw-Hall: London, 1973.
33. Fraunfelder H. *Mössbauer Effect*. W. A. Benjamin: New York, 1963.
34. Bancroft GM, Platt RH. *Adv. Inorg. Chem. Radiochem.* 1972; **15**: 59.
35. Greenwood NN, Gibb TC. *Mössbauer Spectroscopy*. Chapman and Hall: London, 1971.
36. Parish RV. Structure and bonding in tin compounds. In *Mössbauer Spectroscopy Applied to Inorganic Chemistry*, Long GJ (ed.) Vol. 1. Plenum Press: New York, 1984; 527.
37. Clark MG, Maddock AG, Platt RH. *J. Chem. Soc. Dalton Trans.* 1972; 281.
38. Bancroft GM, Kumar Das VG, Sham TK, Clark MG. *J. Chem. Soc. Dalton Trans.* 1976; 643.
39. Casella G, Bertazzi N, Bruschetta G, Pellerito L, Rotondo E, Scopelliti M. *Appl. Organomet. Chem.* 2003; **17**: 932.
40. Daniele PG, De Robertis A, De Stefano C, Gianguzza A, Sammartano S. *J. Chem. Res.* 1990; **(S)300**: (M)2316.
41. Eberson L, Wadsö I. *Acta Chem. Scand.* 1963; **17**: 1552.
42. King EJ. *Acid-Base Equilibria*. Pergamon: New York, 1965.
43. De Robertis A, De Stefano C, Foti C. *J. Chem. Engng Data* 1999; **44**: 262.
44. Jankovics H, Nagy L, Buzás N, Pellerito L, Barbieri R. *J. Inorg. Biochem.* 2002; **92**: 55.
45. Collins RL, Travis JC. The Electric Field Gradient Tensor. In *Mössbauer Effect Methodology*, Gruverman IJ (ed.), Vol. 3. Plenum Press: New York, 1967; 123.
46. Foti C, Gianguzza A, Millero FJ, Sammartano S. *Aquatic Geochem.* 1999; **5**: 381.
47. Daniele PG, Ostacoli G, Rigano C, Sammartano S. *Transition Met. Chem.* 1984; **9**: 385.
48. Capone S, De Robertis A, De Stefano C, Sammartano S. *Talanta* 1986; **33**: 763.

DOI: 10.1002/aoc